Journal of Applied Polymer Science

Surfactant-directed morphology of cross-linked styrene- or vinylbenzyl chloride-based materials

Melpo Karamitrou,[1,2] Efi Sarpaki,[1] Georgios Bokias[1,2]
[1]Department of Chemistry, University of Patras, Patras, GR 26504, Greece
[2]Institute of Chemical Engineering Sciences (ICE/HT-FORTH), Rio-Patras, GR 26504, Greece
Correspondence to: G. Bokias (E-mail: bokias@upatras.gr)

ABSTRACT: Polystyrene (PSt) or poly(vinylbenzyl chloride) (PVBC) crosslinked with divinylbenzyl (DVB) materials were synthesized through free radical polymerization into templates formed by the surfactant polyoxyethylene (4) lauryl ether (Brij-30). The chemical composition of the final products was verified through attenuated total reflectance infrared spectroscopy (ATR-IR) and the thermal behavior was investigated through thermogravimetric analysis (TGA). Depending on the organization of Brij-30 in aqueous solution, three characteristic structures, namely spherical nanoparticles, platelet-like objects and three-dimensional networks, were identified through scanning electron microscopy (SEM) and transmission electron microscopy (TEM). The spherical nanoparticles and the platelet-like objects form rather stable dispersions, especially in aqueous surfactant solutions, as exemplified by the evolution of the turbidity of the PSt-based materials, using sodium dodecyl sulfate as surfactant. All materials retain their integrity even after thermal treatment at high temperature (~200–250°C). The benzyl chloride group of the PVBC-based materials offers a significant potential for further elaboration and practical applications, since they can be further functionalized while retaining their integrity. This potential is demonstrated here through hydrolysis to obtain hydroxyl-functionalized three-dimensional networks. © 2016 Wiley Periodicals, Inc. J. Appl. Polym. Sci. **2016**, *133*, 43297.

KEYWORDS: crosslinking; emulsion polymerization; morphology; self-assembly; surfactants

Received 6 October 2015; accepted 29 November 2015
DOI: 10.1002/app.43297

INTRODUCTION

The self-assembly of surfactants[1] to create hydrophobic and hydrophilic structured domains under varying conditions, such as concentration, temperature, nature of the solvent etc, has been extensively exploited during the last decades for a wide variety of applications. For example, surfactant self-assemblies have been largely applied as templates to create mostly inorganic or metallic nanomaterials,[2–11] as well as to direct the structure of mesoporous materials.[12–24] The properties of such nanostructured products depend on both the nature of its molecular constituents and their precise spatial positioning.

Surfactant templates may also be used for the synthesis of organic (polymeric) nanostructures.[14,25–34] These materials are offered for both traditional, as well as advanced applications. For example, organic nanomaterials offer significant advantages for the preparation of all-organic polymer-based nanocomposites.[35,36] Moreover, adequately functionalized polymeric three-dimensional porous nanostructures (usually prepared through high internal phase emulsions, HIPEs) may find applications as efficient sorbents of chemicals and organic pollutants[37,38] or gases, for example CO_2.[39]

Polymerization in direct, reverse, and bicontinuous microemulsions is the most studied strategy for the surfactant-directed synthesis of organic (polymeric) nanomaterials.[40,41] Typical examples are the latexes obtained when the monomer is polymerized in the dispersed phase of direct or reverse microemulsions. In fact, emulsion polymers derived from styrene (St) monomers are commercially important products.[42] For this reason, the microemulsion (co)polymerization of styrene and other monomers using cationic, nonionic, or anionic surfactants[43–46] has been extensively studied.[47] If the monomer is polymerized in the continuous phase, porous materials may be obtained.[35] In this case, the high internal phase emulsions (HIPEs) are largely applied for the preparation of macroporous materials.[48–52] In fact, the use of surfactants with a low hydrophilic-lipophilic balance (HLB) permits the stabilization of a high volume (more than 74%) internal aqueous phase, acting as the template for the preparation of macroporous crosslinked polymeric materials. For example, sorbitol monooleate (HLB = 4.3[53]) has been widely applied for the

Table I. Feed Composition of Representative Synthetic Experiments

Sample	Brij-30 % (w/v)	Brij-30/ monomers (mol mol^{-1})	St/DVB (mol mol^{-1})	VBC/DVB (mol mol^{-1})	Initiator/ monomers (mol mol^{-1})	Monomer concentration % (w/v)	Temperature (°C)
PSt1	2	1/6.0	3	-	0.02[a]	5	45
PSt2	6	1/5.5	3	-	0.02[a]	10	45
PSt3	13	1/2.5	3	-	0.02[a]	10	50
PVBC1	50	1/0.7	-	3/1	0.02[b]	12	37
PVBC2	13	1/2.5	-	3/1	0.02[a]	13	50
PVBC2-H	*PVBC2/KOH (moles)* 1/4						80

[a] Initiator: KPS/KBS.
[b] Initiator: KPS/TEMED.

preparation of HIPEs based on styrene (St) or 4-vinylbenzyl chloride (VBC).[54]

In bicontinuous microemulsions, the monomer is generally polymerized either in the aqueous phase or in the organic phase.[55,56] Usually, in order to avoid the disruption of the initial microstructure, simultaneous crosslinking is necessary during the polymerization in the organic or aqueous phase of the bicontinuous microemulsion. For example, the polymerization of styrene (St) in the organic phase of a bicontinuous microemulsion leads to a three-dimensional porous solid.[55] On the other hand, the synthesis of two-dimensional polymeric objects requires more sophisticated templates.[35] Thus, the preparation of crosslinked polystyrene nanodisks in the interior of bicelles (discoidal lipid aggregates) with a diameter of 10–40 nm has been reported.[57] Such nanoobjects are interesting as building blocks for polymer-based nanocomposites, since they may result in materials with unusual optical or mechanical properties.

Our aim in the present work was to investigate whether we can modulate the morphology and textural characteristics of polymeric materials through the control of the self-assembly of the surfactant template used. To this end, the surfactant polyoxyethylene (4) lauryl ether (Brij-30) was used. Because the rather high HLB value (HLB = 9.7[58]) is not favorable for the stabilization of HIPEs, we took advantage of the organization of this surfactant into different self-assemblies in aqueous solution, depending on the surfactant concentration and temperature. In fact, for the surfactant concentrations applied in the present study, Brij-30 is expected to form micellar, lamellar, or sponge phases.[59] As representative examples, the polymerization of styrene (St) or 4-vinylbenzyl chloride (VBC) in the presence of the crosslinker divinylbenzyl (DVB) into these Brij-30 templates was explored. The use of DVB allows to the product to retain the possible textures after the removal of the template. PSt was chosen as a typical synthetic polymer, while the chlorine-functionalization in the case of PVBC can potentially lead to functional organic materials of controlled morphologies.[37,60–63] To demonstrate this possibility, we proceeded to the hydrolysis of selected PVBC products, aiming at respective hydroxyl-functionalized products.

EXPERIMENTAL

Materials

The monomers, styrene (St, 99%), 4-vinylbenzyl chloride (VBC, 90%), and divinylbenzene (DVB, 80%) were purchased from Aldrich. The emulsifiers polyoxyethylene (4) lauryl ether [Brij-30 or Brij L4)] and sodium dodecyl sulfonate (SDS) as well as the initiators, potassium persulfate (KPS, 99%), potassium metabisulfate (KBS, 98%), and tetramethylethylenediamine (TEMED, 99%), were also obtained from Aldrich. The solvent tetrahydrofuran (THF, 99.9%) was purchased from Aldrich whereas chloroform (99.97%) was purchased from Fisher Chemicals. Ultrapure 3D-water was obtained using a SG Waters apparatus.

Polymerizations

The conditions applied for the synthetic trials for both crosslinked PVBC samples and crosslinked PSt samples are summarized in Table I. As a representative example, the synthesis of PSt3 is given:

In a three-neck 100-mL round bottom flask equipped with a reflux condenser and a magnetic stirrer, 27 mL of 3D H_2O and 4.0 mL (10.4×10^{-3}mol) of the emulsifier Brij-30 were added. The solution was degassed with nitrogen for 30 min. At the same time the organic phase was prepared in a conical flask by the addition of 2.4 mL (20.9×10^{-3}mol) of St and 1.0 mL (7.0×10^{-3}mol) of the crosslinker DVB. Afterward, the mixture of both the aqueous and the organic phases was vigorously stirred with a magnetic stirrer for 1 h. At a next step, the redox couple of KPS/KBS initiators (2% on monomers moles) was added, 0.149 g (0.55×10^{-3}mol) of KPS and 0.124 g (0.55×10^{-3} mol) of KBS, dissolved in 3 mL of 3D H_2O. The emulsion polymerization took place at 50°C. The reaction was left under stirring overnight and the final product was obtained through vacuum filtration, washing with 3D H_2O and ethanol and drying under vacuum at 40°C.

Moreover, the linear homopolymer PVBC was synthesized through typical free radical polymerization in organic solvent at 80°C, whereas the linear homopolymer PSt was synthesized through emulsion polymerization at 80°C using sodium dodecyl sulfate as emulsifier.

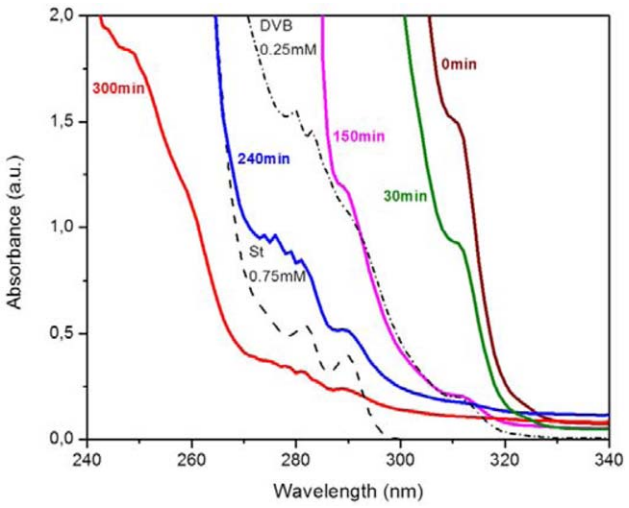

Figure 1. UV–vis spectra of St (0.75 m*M*), DVB (0.25 m*M*), and the reaction medium of PSt2 after 0, 30, 150, 240, and 300 min of polymerization. [Color figure can be viewed in the online issue, which is available at wileyonlinelibrary.com.]

Hydrolysis of PVBC2

In a 100-mL round bottom flask equipped with a reflux condenser and a magnetic stirrer, 50 mL of ethanol, 1.5 g of PVBC2 powder, and 14.5 mL (29.2×10^{-3}mol KOH) of a 2*M* KOH solution in methanol were added. The temperature was set at 80°C and the mixture was left under these conditions for 2 days. The product was obtained by vacuum filtration, washing with 3D H_2O and drying under vacuum at 70°C.

Characterization Techniques

Thermogravimetric Analysis (TGA). Thermogravimetric analysis was performed on a Setaram Labsys^{TM} TG instrument under a nitrogen atmosphere. For the measurements, 5–10 mg of a solid sample were placed in a platinum holder and were heated under constant nitrogen flow up to 800°C and at a temperature ramp of 20°C min^{-1}.

Attenuated Total Reflection Infrared Spectroscopy (ATR-IR). Compositional and chemical characteristics were evaluated by recording infrared spectra of a solid sample, using a "Bruker Optics' Alpha-P Diamond ATR Spectrometer of Bruker Optics GmbH."

Scanning Electron Microscope (SEM). Scanning electron micrographs were recorded using a LEO SUPRA 35VP electron microscope operating at 15 kV. All the samples were sputter-coated with an Au film to reduce charging.

Transmission Electron Microscopy (TEM). A JEM 2100 instrument at an electron acceleration voltage of 200 kV was employed for the measurements. TEM samples were prepared by drying a drop of a dispersion of the sample (~0.01 wt %) in chloroform, on a carbon coated copper grid.

Electrophoresis and Dynamic Light Scattering (DLS). The zeta potential (ζ) and size of the samples were explored using electrophoresis and DLS measurements which were performed at 25°C by means of a NanoZetasizer, Nano ZS Malvern apparatus. The excitation light source was a 4 mW He–Ne laser at 633 nm and the intensity of the scattered light was measured at 173°.

UV Spectroscopy. The progress of the polymerization was monitored using a UV 1800 Hitachi UV–vis spectrophotometer. In these studies, small aliquots (25 μL) were withdrawn from the reaction mixture at regular intervals (30 min) and diluted with 5 mL of THF.

RESULTS AND DISCUSSION

Synthesis and Characterization of Crosslinked PSt and PVBC Materials

As previously discussed, the synthesis of crosslinked PSt and PVBC of controlled morphology was attempted in templates of Brij-30 at various concentrations. Three PSt and two PVBC

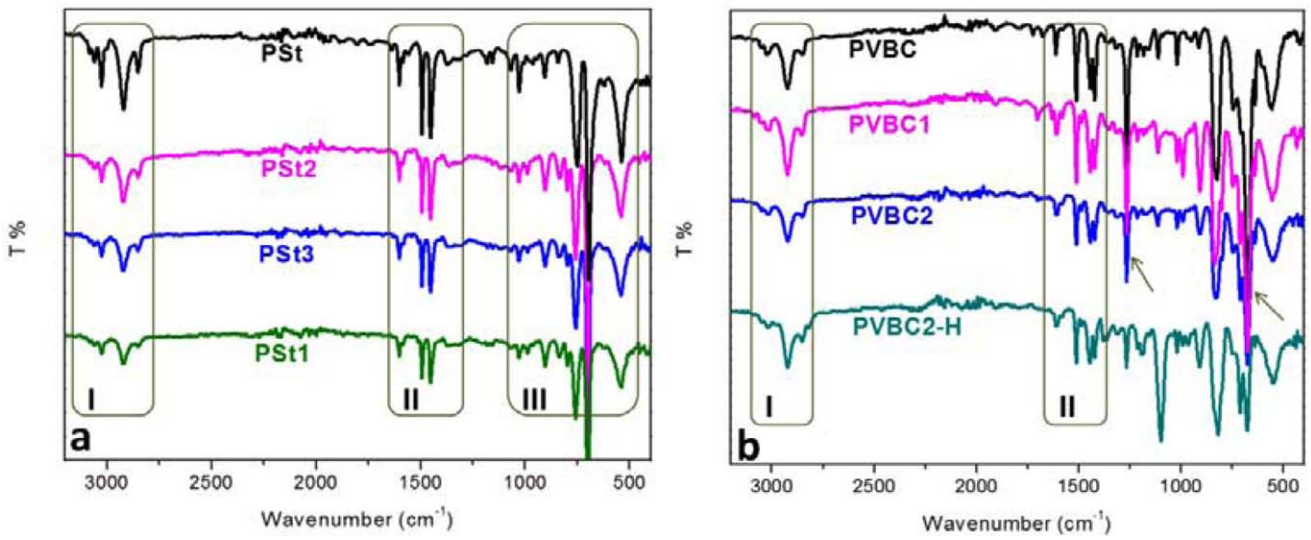

Figure 2. ATR-IR spectra of (a) PSt, PSt1, PSt2, and PSt3 and (b) PVBC, PVBC1, PVBC2, and PVBC2-H. [Color figure can be viewed in the online issue, which is available at wileyonlinelibrary.com.]

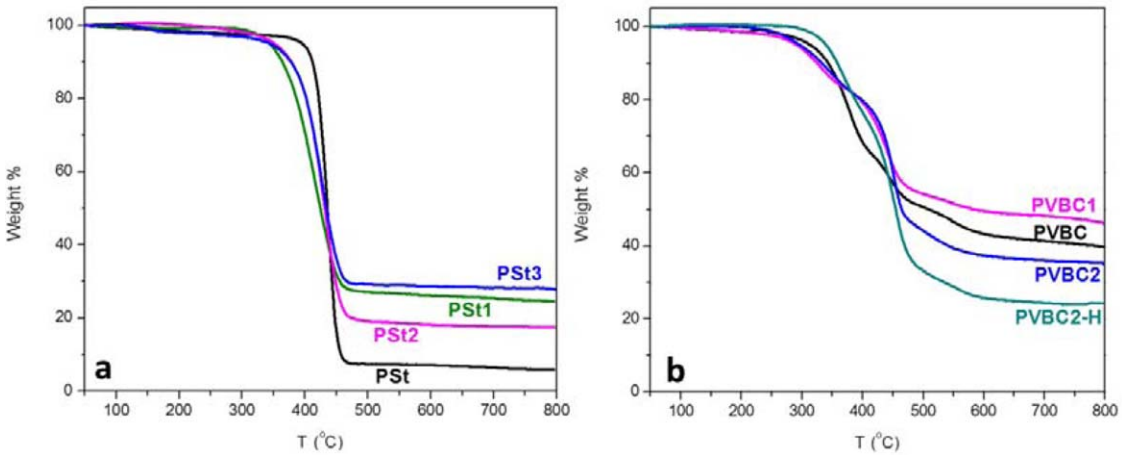

Figure 3. TGA results for (a) PSt, PSt1, PSt2, and PSt3 and (b) PVBC, PVBC1, PVBC2, and PVBC2-H. [Color figure can be viewed in the online issue, which is available at wileyonlinelibrary.com.]

samples were prepared for the present investigation. Moreover, one PVBC sample (PVBC2) was hydrolyzed in order to obtain the hydroxyl-functionalized sample, PVBC2-H. Table I summarizes the materials synthesized as well as the synthetic conditions applied.

The progress of polymerizations was monitored through UV–vis spectroscopy. Representative UV–vis spectra for the polymerization of sample PSt2 are shown in Figure 1.

The spectra of dilute solutions of the monomer St and the crosslinker DVB in THF are also given in Figure 1, for reasons of comparison. Under these concentration conditions, the vinylic bonds of the monomers lead to the observation of absorption peaks in the region 280–290 nm for St and of a shoulder at ~310 nm for DVB. It is evident, especially for DVB, that these peaks gradually get weaker and finally disappear with the reaction time, as a consequence of the polymerization of the vinylic bonds. In fact, these results suggest that practically all monomers have been polymerized within roughly 6 h.

The chemical composition and the complete purification of the materials have been verified through attenuated total reflection infrared spectroscopy, ATR-IR. The spectra of the crosslinked PSt and PVBC samples are presented in Figure 2(a,b), respectively, and they are compared with those of the two homopolymers, PSt and PVBC. More specifically, for all PSt samples [Figure 2(a)], the characteristic peaks in the region 3070–2850 cm^{-1} are observed (region I), corresponding to the C—H alkene. Moreover, the peaks within the region II and III, 1600–1370 cm^{-1} and 1030–538 cm^{-1}, respectively, correspond to the C=C stretch, C—C stretch and C—H stretch of the aromatic structure of polystyrene.[64] In addition to the aforementioned peaks, the characteristic peaks of PVBC are also evident in the spectra of Figure 2(b). Thus, the characteristic peaks of C—H are observed in the region I, whereas those of C=C aromatic rings can be seen in region II, 1610–1419 cm^{-1}. Moreover, the peaks at 1265 and 673 cm^{-1} are attributed to the stretching vibration of the bond C—Cl.[65] These peaks are hardly observed in the case of the hydrolyzed sample PVBC2-H, while a new peak at 1100 cm^{-1} is observed, corresponding to stretching vibration of the C—O bond, indicating the success of hydrolysis.

The thermal stability was investigated through thermogravimetric analysis (TGA) under nitrogen atmosphere (Figure 3). The TGA curves show that all crosslinked PSt samples [Figure 3(a)] are thermally stable up to ~370°C and then they decompose sharply, leaving a rather low char (~20%) at high temperatures. The thermal stability of the PVBC samples [Figure 3(b)], on the other hand, is somewhat weaker and they start to decompose at ~280°C. For these materials, two decomposition steps are observed. Possibly, the first step reflects the decomposition of the C—Cl groups (or, the C—OH groups in the case of the hydrolyzed PVBC2-H sample). Moreover, hydrolysis seems not to influence the thermal stability of the material, since the decomposition of PVBC2 and PVBC2-H starts roughly at the same temperature. However, PVBC2-H leaves a rather lower char at high temperatures, as compared to PVBC2.

Morphology Control of Crosslinked Polymeric Materials

As already mentioned the most possible assemblies formed by Brij-30 are micellar, lamellar, and sponge phase, depending on concentration.[1] These self-assembled structures were used as templates for the polymerization of St and VBC (Table II). The morphology of the samples was investigated through scanning electron microscopy (SEM) and transmission electron microscopy (TEM). Representative images of the three PSt samples are presented in Figure 4. Observing the images, it is evident that

Table II. Self-organization of Brij-30 in Aqueous Solution and Morphology of Crosslinked PSt and PVBC Structures Formed

Brij-30; w/v %	Possible self-assembly of Brij-30	Morphology of the product
2	Micelle	Spheres
6	Lamellar	Platelet-like
13	Sponge	Network
50	Lamellar	Platelet-like

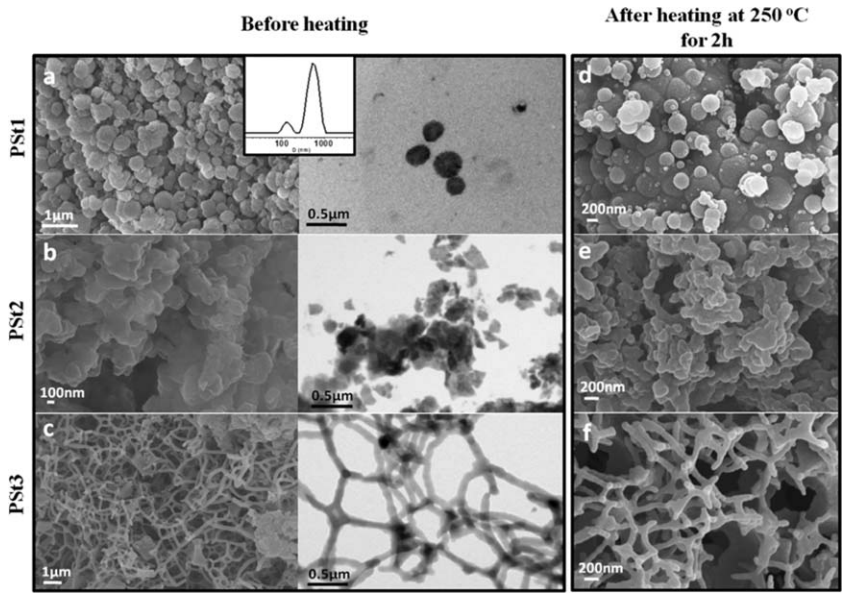

Figure 4. SEM (left) and TEM (middle) images of PSt1, (a), PSt2 (b), and PSt3 (c). The scale bar is 0.5 μm for TEM images, and for SEM images is (a) 1 μm, (b) 0.1 μm and (c) 1 μm. SEM (right) images of PSt1 (d), PSt2 (e), PSt3 (f) after heating at 250°C for 2 h. The scale bar is 200 nm. The DLS of PSt1 (0.002%w/v in aqueous 5 m*M* SDS solution) are also shown in (a).

the surfactant concentration is indeed decisive to direct the morphology of the cross-linked St-based materials obtained.

At low surfactant concentration (2% (w/v)), the templates for polymerization of St are the spherical micelles of Brij-30. In fact, this apparently leads to the formation of a direct oil-in-water emulsion. As a consequence, spherical crosslinked PSt nanoparticles are observed through SEM and TEM for the sample PSt1 [Figure 4(a)]. The mean size is about 150–200 nm. Nevertheless, larger particles, as well as aggregates of nanoparticles, are also clearly observable. This is further verified through the dynamic light scattering (DLS) study shown in the inset of Figure 4(a). For this study, a 0.002% dispersion of PSt1 in aqueous 5 m*M* SDS solution was used (see also, the discussion of Figure 5). In accordance with the SEM investigation, two populations with sizes ~150 and ~600 nm are detected through DLS.

At the intermediate Brij-30 concentration (6%(w/v)), the template is the lamellar structure formed by the surfactant and the morphology of the crosslinked polymers changes to platelet-like [Figure 4(b)], sample PSt2. Although it is not possible to get accurate estimations on the three-dimensional size of the structures observed through SEM and TEM, it is rather evident that the depth of these objects is considerably smaller than the other two dimensions. The shape of these practically two-dimensional platelet-like objects is irregular. Moreover, while their depth is probably of the order of some tenths of nanometers, these structures are rather large, since the other two dimensions are of the order of 200–300 nm up to a few micrometers.

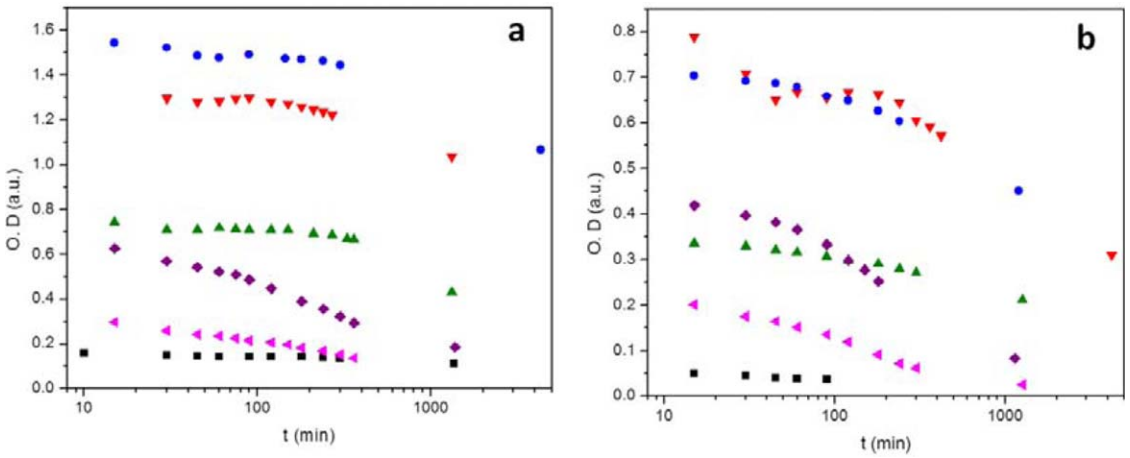

Figure 5. Turbidity of dispersion of (a) PSt1 and (b) PSt2, in chloroform at concentrations 0.01%w/v (◀) and 0.02%w/v (♦), in aqueous solution of 5 m*M* SDS at concentrations 0.002%w/v (■) and 0.02%w/v (●) and in aqueous solution of 30 m*M* SDS at concentrations 0.01%w/v (▲) and 0.02%w/v (▼). [Color figure can be viewed in the online issue, which is available at wileyonlinelibrary.com.]

Table III. ζ-potential and Size of PSt1 Samples Dispersed in Aqueous SDS Solutions through Dynamic Light Scattering (DLS) Study

	PSt1			
	5 mM SDS		30 mM SDS	
	0.002% w/v	0.02% w/v	0.01% w/v	0.02% w/v
Size (nm)	570 (90%)	600 (93%)	600 (100%)	715 (92%)
	130 (10%)	140 (7%)	-	170 (8%)
ζ-potential (mV)	−46.8	−47.1	−61.9	−62.9

Finally, at the higher surfactant concentration [13%(w/v)], the surfactant self-assembles into sponge structures and a three-dimensional crosslinked PSt network is formed [Figure 4(c)], sample PSt3. In contrast, to the respective PSt HIPEs, these networks are consisted by crosslinked rod-shaped objects. The width of these rods is ∼50 nm, while their length varies from hundreds nanometers up to a few micrometers.

In all cases, the influence of thermal treatment on the aforementioned objects was evaluated. As seen in Figure 4(d–f), all samples retain essentially their morphology and textural characteristics after thermal treatment at 250°C for 2h under inert atmosphere.

With the exception of the crosslinked PSt network (sample PSt3), the other two morphologies (nanoparticles and platelet-like objects) could potentially be dispersible. Thus, the dispersibility of PSt1 and PSt2 was checked both in an organic solvent namely chloroform, as well as in aqueous sodium dodecyl sulfate (SDS) solutions. The concentrations of the dispersions ranged within 0.0025–0.02% (w/v), while the concentration of SDS was chosen to be either 30 mM (well above the critical micelle concentration, cmc, of SDS, 8 mM^{1}) or 5 mM (below cmc). All suspensions were prepared by the addition of solid samples in the SDS or chloroform solution using a bath sonicator for 10 min. The evolution with time of the optical density of the suspensions was monitored, as a simple criterion of stability (Figure 5). Interestingly, the turbidity of the dispersions of PSt2 is generally lower than that of the sample PSt1 under the same concentration and solvent conditions. Moreover, it is noteworthy that the turbidity of the dispersions in chloroform is clearly lower than that of the dispersions in aqueous SDS solutions. However, it seems that the SDS concentration does not influence significantly the turbidity levels, suggesting that SDS do associate with and effectively stabilize in the aqueous environment these hydrophobic objects even at a concentration below cmc. This is also supported by the large negative ζ-potential values (from −45 down to −60 mV), determined in all cases (Table III). From the evolution with time of the turbidity it is evident that the dispersions in aqueous SDS solutions are more stable than those in chloroform. In fact, the optical density of the dispersions in chloroform decreases continuously with time, suggesting precipitation of the samples. In contrast, the optical density of the dispersions in aqueous SDS solutions remain rather constant for at least 5–6 h, while it is maintained in some cases at comparable levels even after ∼24 h.

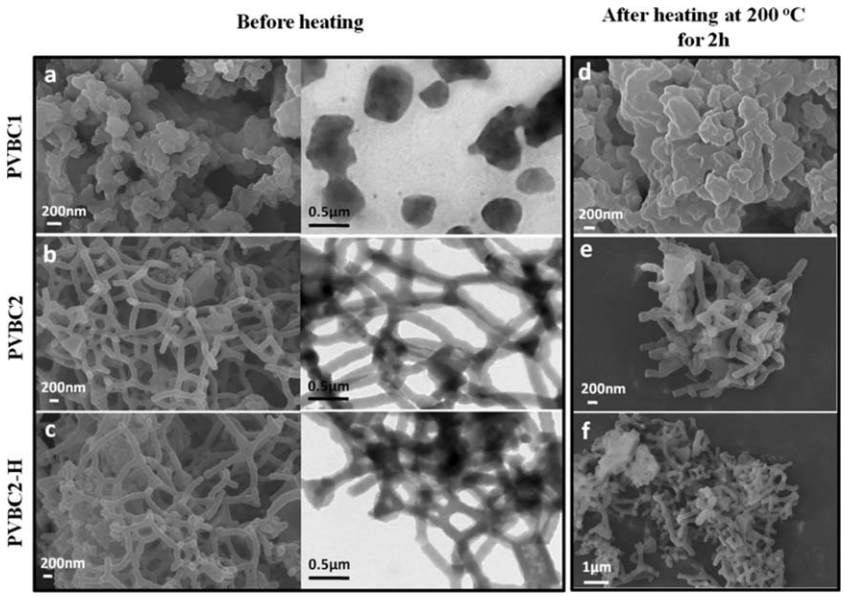

Figure 6. SEM (left) and TEM (middle) images of crosslinked PVBC1 (a), PVBC2 (b) and PVBC2-H (c). The scale bar is 200 nm for SEM images and 0.5 μm for TEM images. SEM (right) images of PVBC1 (d), PVBC2 (e), PVBC2-H (f) after heating at 200°C for 2 h. The scale bar is 1, 0.5, and 1 μm, respectively.

In the case of PVBC, the lamellar and sponge phase of Brij-30 in aqueous solution were chosen as templates for the polymerization. Just like PSt, platelet-like objects (sample PVBC1) and three-dimensional crosslinked PVBC networks (sample PVBC2) are obtained, respectively, as revealed from the SEM and TEM investigation (Figure 6). Moreover, the texture of the network remains intact even after hydrolysis to obtain the respective hydroxyl-functionalized material (sample PVBC2-H). Finally, the microscopic investigation of these samples after heating at 200°C for 2 h reveals that they retain their morphology.

CONCLUSIONS

This work focused on synthesizing crosslinked polymeric materials with controlled morphology/texture using surfactant templates. The polymerization of St (in the presence of a crosslinker) was used as a representative case, while the self-assemblies formed by the surfactant Brij-30 in aqueous solutions (micellar, lamellar, and sponge phase) were the polymerization templates. The polymerization of VBC was also investigated as an alternative case of an easily functionalized material with well-defined structure.

Depending on surfactant concentration, SEM and TEM characterization reveals that the resulting crosslinked polymeric materials may obtain three distinguished morphologies, namely spherical nanoparticles, platelet-like objects or three-dimensional networks. While the first morphology (spherical nanostructures) is rather trivial and it can be achieved through typical emulsion polymerizations, the other two textures (platelet-like objects and three-dimensional networks) are rarely observed and they offer a significant potential for further elaboration and practical applications. For example, the platelet-like structures may be used for the preparation of polymer-based nanocomposites with novel or improved properties, whereas the three-dimensional networks offer the potential for the elaboration of novel sorbent materials, as alternative to HIPEs.

Concerning potential applications, the importance of the VBC-based materials should be stressed. In the present work, the hydroxyl-functionalization has been demonstrated through hydrolysis, as a simple example. Nevertheless, the benzyl-chloride group offers many possibilities for functionalization, such as introduction of quaternary nitrogen groups, initiation of atom transfer radical polymerizations, etc. Moreover, the synthetic methodology for the preparation of such materials can be easily adapted, for example through using porogenic solvents or performing post-polymerization reactions, in order to induce porosity and/or to improve mechanical properties, depending on the desired application.

ACKNOWLEDGMENTS

The research leading to these results has received funding from the European Union's Seventh Framework Programme (FP7/2012-2016) under the grant agreement no. 280759, NanoBarrier entitled. "Extended shelf-life biopolymers for sustainable and multifunctional food packaging solutions." The authors thank Dr Maria Kollia from the Lab of Electron Microscopy and Microanalysis at the University of Patras and Dr Vasilis Drakopoulos from the Institute of Chemical Engineering Sciences (ICE/HT-FORTH) for the TEM and SEM images, respectively.

REFERENCES

1. Holmberg, K.; Jonsson, B.; Kronberg, B.; Lindman, B. Surfactants and Polymers in Aqueous Solution, 2nd ed.; Wiley: Chichester, **2003**.
2. Soten, I. G.; Ozin, A. *Curr. Opin. Colloid Interface Sci.* **1999**, *4*, 325.
3. Soler-Illia, G. J.; de, A. A.; Sanchez, C.; Lebeau, B.; Patarin, J. *Chem. Rev.* **2002**, *102*, 4093.
4. Pileni, M. P. *Nat. Mater.* **2003**, *2*, 145.
5. Holmberg, K. *J. Colloid Interface Sci.* **2004**, *274*, 355.
6. Eastoe, J.; Hollamby, M. J.; Hudson, L. *Adv. Colloid Interface Sci.* **2006**, *128–130*, 5.
7. Brinker, C. J.; Dunphy, D. R. *Curr. Opin. Colloid Interface Sci.* **2006**, *11*, 126.
8. Wang, C.; Chen, D.; Jiao, X. *Sci. Technol. Adv. Mater.* **2009**, *10*, 023001.
9. Qi, L. *Coord. Chem. Rev.* **2010**, *254*, 1054.
10. Vigderman, L.; Khanal, B. P.; Zubarev, E. R. *Adv. Mater.* **2012**, *24*, 4811.
11. Sorrenti, A.; Illa, O.; Ortuno, R. M. *Chem. Soc. Rev.* **2013**, *42*, 8200.
12. Okay, O. *Prog. Polym. Sci.* **2000**, *25*, 711.
13. Antonietti, M. *Curr. Opin. Colloid Interface Sci.* **2001**, *6*, 244.
14. John, V. T.; Simmons, B.; McPherson, G. L.; Bose, A. *Curr. Opin. Colloid Interface Sci.* **2002**, *7*, 288.
15. Patarin, J.; Lebeau, B.; Zana, R. *Curr. Opin. Colloid Interface Sci.* **2002**, *7*, 107.
16. Palmqvist, A. E. C. *Curr. Opin. Colloid Interface Sci.* **2003**, *8*, 145.
17. Kimura, T. *Microporous Mesoporous Mater.* **2005**, *77*, 97.
18. Berggren, A.; Palmqvist, A. E. C.; Holmberg, K. *Soft Matter* **2005**, *1*, 219.
19. Shi, Y.; Wan, Y.; Zhao, D. *Chem. Soc. Rev.* **2011**, *40*, 3854.
20. Meng, X.; Nawaz, F.; Xiao, F. S. *Nano Today* **2009**, *4*, 292.
21. Gokmen, M. T.; Prez, F. E. D. *Prog. Polym. Sci.* **2012**, *37*, 365.
22. Shiba, K.; Tagaya, M.; Tilley, R. D.; Hanagata, N. *Sci. Technol. Adv. Mater.* **2013**, *14*, 023002.
23. Pal, N.; Bhaumik, A. *Adv. Colloid Interface Sci.* **2013**, *189/190*, 21.
24. Sterchele, S.; Centomo, P.; Zecca, M.; Hanková, L.; Jerábek, K. *Microporous Mesoporous Mater.* **2014**, *185*, 26.
25. Eastoe, J.; Warne, B. *Curr. Opin. Colloid Interface Sci.* **1996**, *1*, 800.
26. Antonietti, M.; ltner, C. G.; Hentze, H. P. *Langmuir* **1998**, *14*, 2670.
27. Hentze, H. P.; Antonietti, M. *Curr. Opin. Solid State Mater. Sci.* **2001**, *5*, 343.
28. Hentze, H. P.; Antonietti, M. *Rev. Mol. Biotechnol.* **2002**, *90*, 27.

29. Hentze, H. P.; Kaler, E. W. *Curr. Opin. Colloid Interface Sci.* **2003**, *8*, 164.
30. Hentze, H. P.; Kaler, E. W. *Chem. Mater.* **2003**, *15*, 708.
31. Becerra, F. J.; Soltero, F. A.; Puig, J. E.; Schulz, P. C.; Esquena, J.; Solans, C. *Colloid. Polym. Sci.* **2003**, *282*, 103.
32. Yan, F.; Texter, J. *Adv. Colloid Interface Sci.* **2006**, *128–130*, 27.
33. Walker, L. M.; Kuntz, D. M. *Curr. Opin. Colloid Interface Sci.* **2007**, *12*, 101.
34. Miloševic, I.; Mauroy, V.; Dabboue, H.; Serieye, S.; Warmont, F.; Salvetat, J. P.; Saboungi, M. L.; Guillot, S. *Microporous Mesoporous Mater.* **2009**, *120*, 7.
35. Tekobo, S.; Richter, A. G.; Dergunov, S. A.; Pingali, S. V.; Urban, V. S.; Yan, B.; Pinkhassik, E. *J. Nanopart. Res.* **2011**, *13*, 6427.
36. Martín, J.; Maiz, J.; Sacristan, J.; Mijangos, C. *Polymer* **2012**, *53*, 1149.
37. Krajnc, P.; Brown, J. F.; Cameron, N. R. *Org. Lett.* **2002**, *4*, 2497.
38. Huang, J.; Wub, X.; Zha, H.; Yuan, B.; Deng, S. *Chem. Eng. J.* **2013**, *218*, 267.
39. He, H.; Li, W.; Lamson, M.; Zhong, M.; Konkolewicz, D.; Hui, C. M.; Yaccato, K.; Rappold, T.; Sugar, G.; David, N. E.; Damodaran, K.; Natesakhawat, S.; Nulwala, H.; Matyjaszewski, K. *Polymer* **2014**, *55*, 385.
40. Rao, J. P.; Geckeler, K. E. *Prog. Polym. Sci.* **2011**, *36*, 887.
41. Bourcier, S.; Vancaeyzeele, C.; Vidal, F.; Fichet, O. *Polymer* **2013**, *54*, 4436.
42. Bahattad, M. A. *J. Appl. Polym. Sci.* **2011**, *121*, 2535.
43. Atik, S.; Thomas, J. K. *J. Am. Chem. Soc.* **1983**, *105*, 4515.
44. Aguiar, A.; Gonzalez-Villegas, S.; Rabelero, M.; Mendizabal, E.; Puig, J. E. *Macromolecules* **1999**, *32*, 6767.
45. Garay-Jimenez, J. C.; Gergeresa, D.; Young, A.; Lim, D. V.; Turos, E. *Nanomed. Nanotechnol. Biol. Med.* **2009**, *5*, 443.
46. Ziegler, A.; Landfester, K.; Musyanovych, A. *Colloid. Polym. Sci.* **2009**, *287*, 1261.
47. Tieke, B. *Colloid. Polym. Sci.* **2005**, *283*, 421.
48. Sevsek, U.; Krajnc, P. *React. Funct. Polym.* **2012**, *72*, 221.
49. Sevsek, U.; Brus, J.; Jerabek, K.; Krajnc, P. *Polymer* **2014**, *55*, 410.
50. Silverstein, M. S. *Prog. Polym. Sci.* **2014**, *39*, 199.
51. Silverstein, M. S. *Polymer* **2014**, *55*, 304.
52. Tebboth, M.; Menner, A.; Kogelbauer, A.; Bismarck, A. *Curr. Opin. Chem. Eng.* **2014**, *4*, 114.
53. Silverstein, M. S.; Cameron, N. R.; Hillmyer, M. A. Porous Polymers; Wiley: New Jersey, **2011**.
54. Audouin, F.; Heise, A. *Polymer* **2014**, *55*, 403.
55. Sasthav, M.; Cheung, H. M. *Langmuir* **1991**, *7*, 1378.
56. Liu, J.; Teo, W. K.; Chew, C. H.; Gan, L. M. *J. Appl. Polym. Sci.* **2000**, *77*, 2785.
57. Glover, K. J.; Whiles, J. A.; Wu, G.; Yu, N.; Deems, R. *Biophys. J.* **2001**, *81*, 2163.
58. Tan, A. L.; Laili, C. R.; Hamdan, S.; Doreen, S. H. *J. Sci. Technol.* **2009**, *1*, 1.
59. Mitchell, D. J.; Tiddy, G. J. T.; Waring, L.; Bostock, T.; MacDonald, M. P. *J. Chem. Soc. Faraday Trans. 1* **1983**, *79*, 975.
60. Schoo, H. F. M.; Challa, G. *React. Polym.* **1992**, *16*, 125.
61. Benicewicz, B. C.; Jarvinen, G. D.; Kathios, D. J.; Jorgensen, B. S. *Radioanal. J. Nucl. Chem.* **1998**, *235*, 31.
62. Stefanec, D.; Krajnc, P. *React. Funct. Polym.* **2005**, *65*, 37.
63. Li, W.; Zhang, W.; Dong, X.; Yan, L.; Qi, R.; Wang, W.; Xie, Z.; Jing, X. *J. Mater. Chem.* **2012**, *22*, 17445.
64. Radhi, M. M.; Tan, W. T.; Rahman, M. Z. B. A.; Kassim, A. B. *Sci. Res. Essays* **2012**, *7*, 790.
65. Koromilas, N. D.; Lainioti, G. C.; Oikonomou, E. K.; Bokias, G.; Kallitsis, J. K. *Eur. Polym. J.* **2014**, *54*, 39.